**Supplementary Information**

# Chemical Pre-regulation of 2D Perovskite Nucleation Enables Phase-Homogeneous 2D/3D Perovskite Interfaces

*Bin Wu[a,b], Di Shen[a], Jiaxue Zhai[a,b], Jiayan Chen[a,b], YongHua[a,b], Chong Wang[a,b], Shafidah Shafian[c,*], Lin Xie[a,b,*]*

a. School of Materials and Energy, Yunnan University, Kunming, 650091, China

b. International Joint Research Center for Optoelectronic and Energy Materials, Yunnan University, Kunming, 650091, China

c. Solar Energy Research Institute, Universiti Kebangsaan Malaysia, Bangi, Selangor, 43600, Malaysia

*Corresponding Author e-mail: lxie@ynu.edu.cn, norshafidah@ukm.edu.my

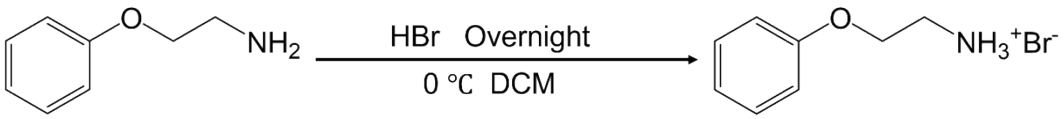


**Scheme S1**. The synthesis route of PEOABr.

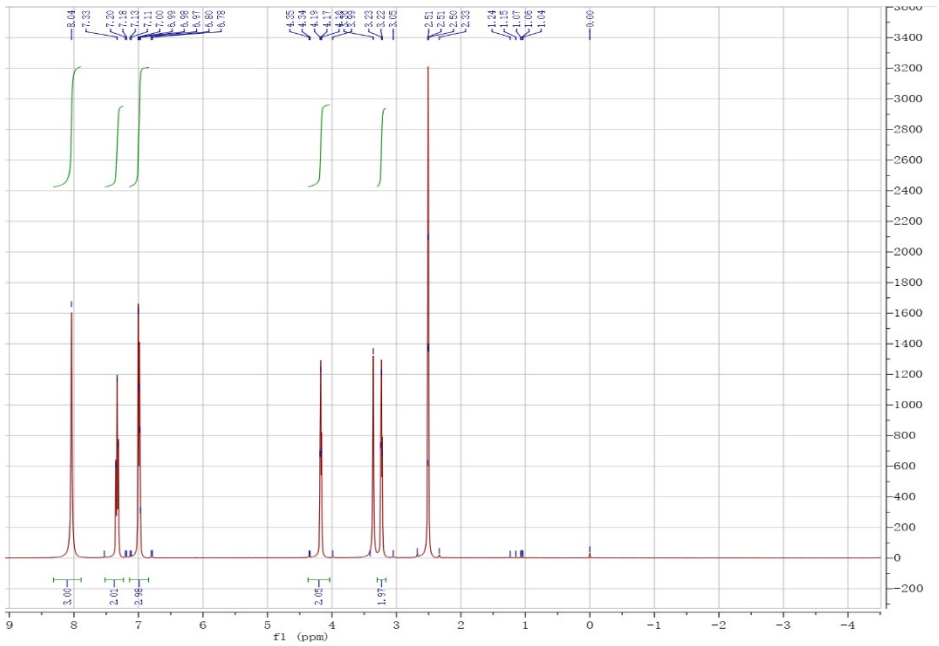


**Figure S1**. $^{1}$H NMR spectra of PEOABr.

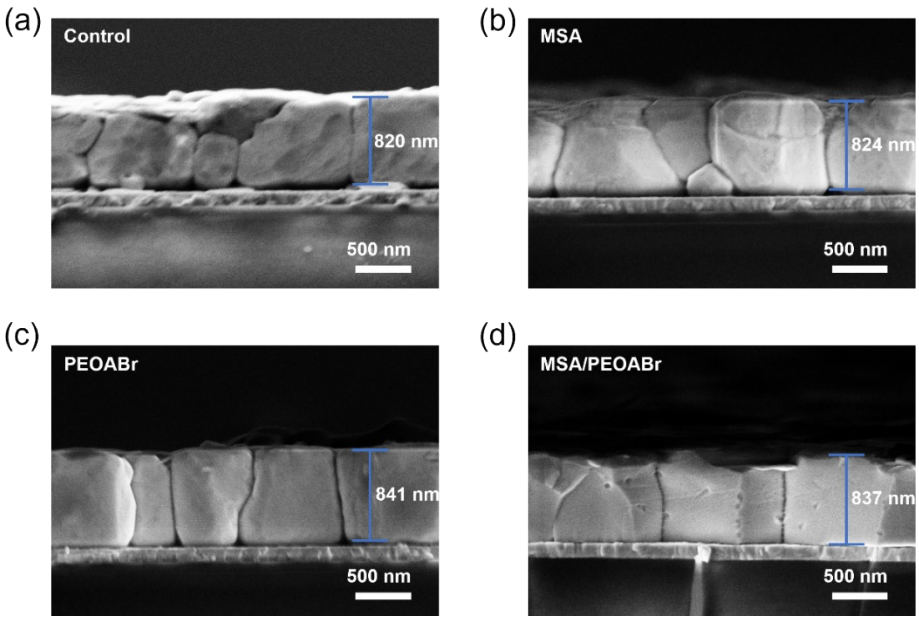


**Figure S2.** Cross-sectional SEM images of perovskite films with different surface-treatment conditions: (a) Control, (b) MSA, (c) PEOABr, and (d) MSA/PEOABr.

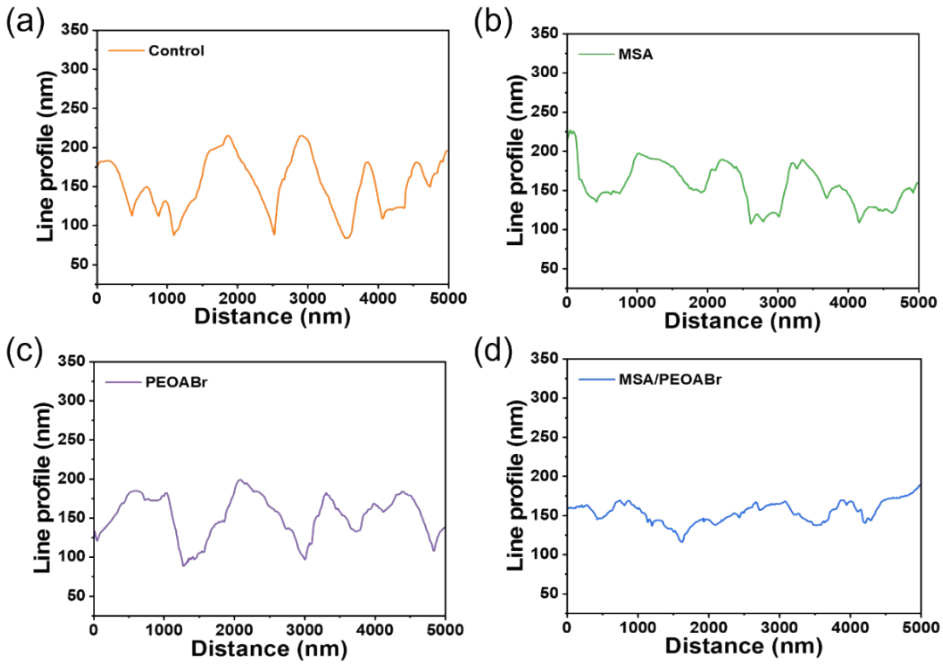


**Figure S3.** (a-d) Line profiles corresponding to the AFM images in Figure 1 (g-j).

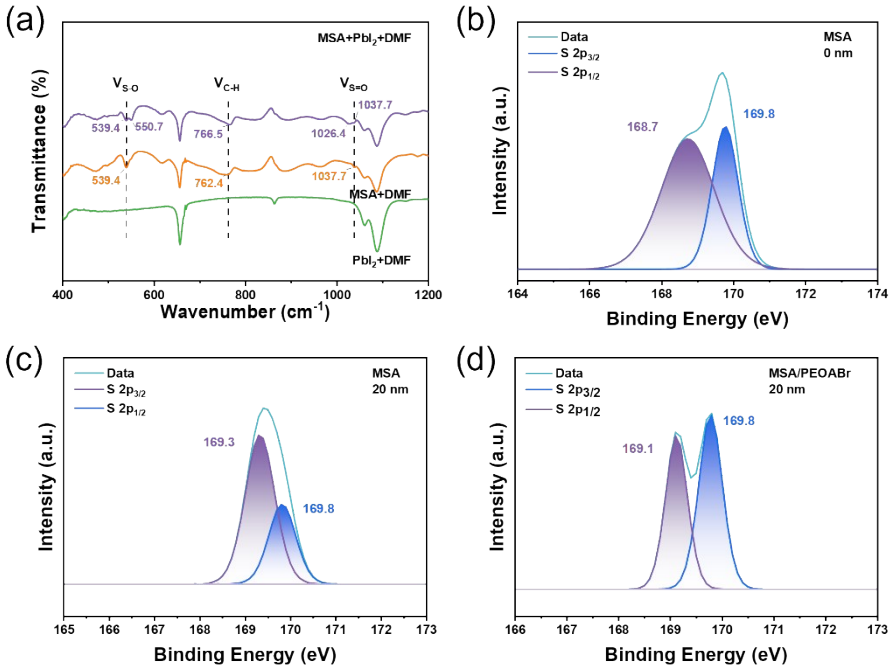


**Figure S4.** (a) FTIR spectra of $PbI_2$+DMF, MSA+DMF, and MSA+$PbI_2$+DMF. (b–d) High-resolution S 2p XPS spectra with peak fitting for MSA (0 nm), MSA (20 nm), and MSA/PEOABr (20 nm), respectively.

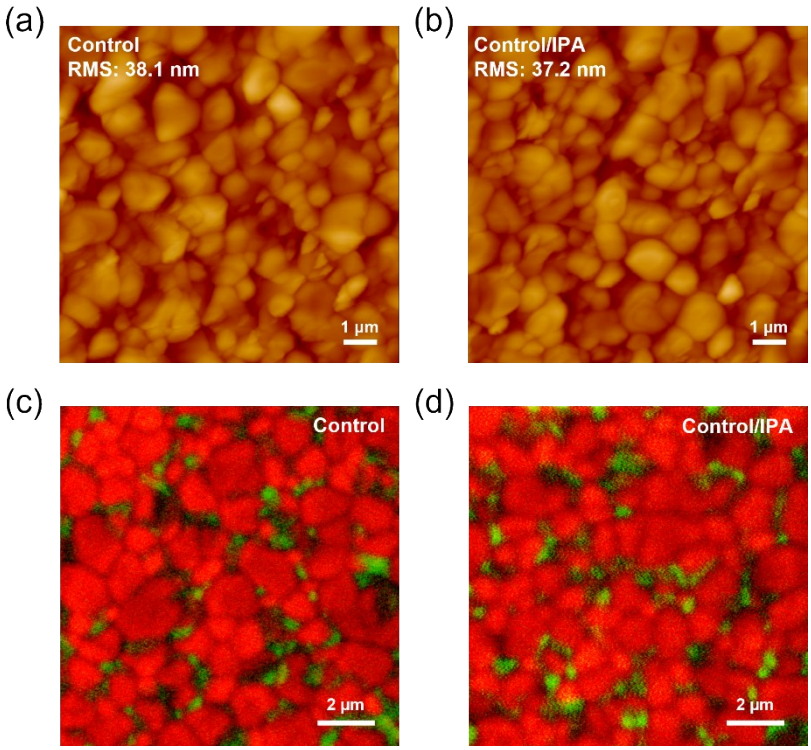


**Figure S5.** (a,b) AFM topography images of the Control and Control/IPA perovskite films. (c,d) CLSM mapping images of the Control and Control/IPA films.

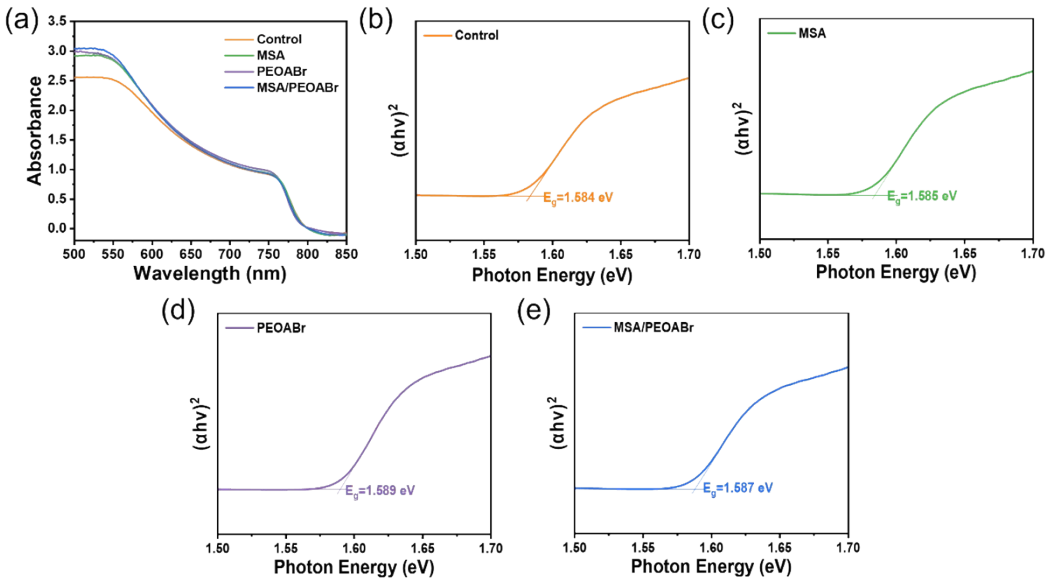


**Figure S6.** (a) The UV-vis spectra of perovskite films prepared with interface treatment using MSA, PEOABr, the combined MSA/PEOABr, and without any treatment. (b-e) Tauc plots for optical bandgap fitting.

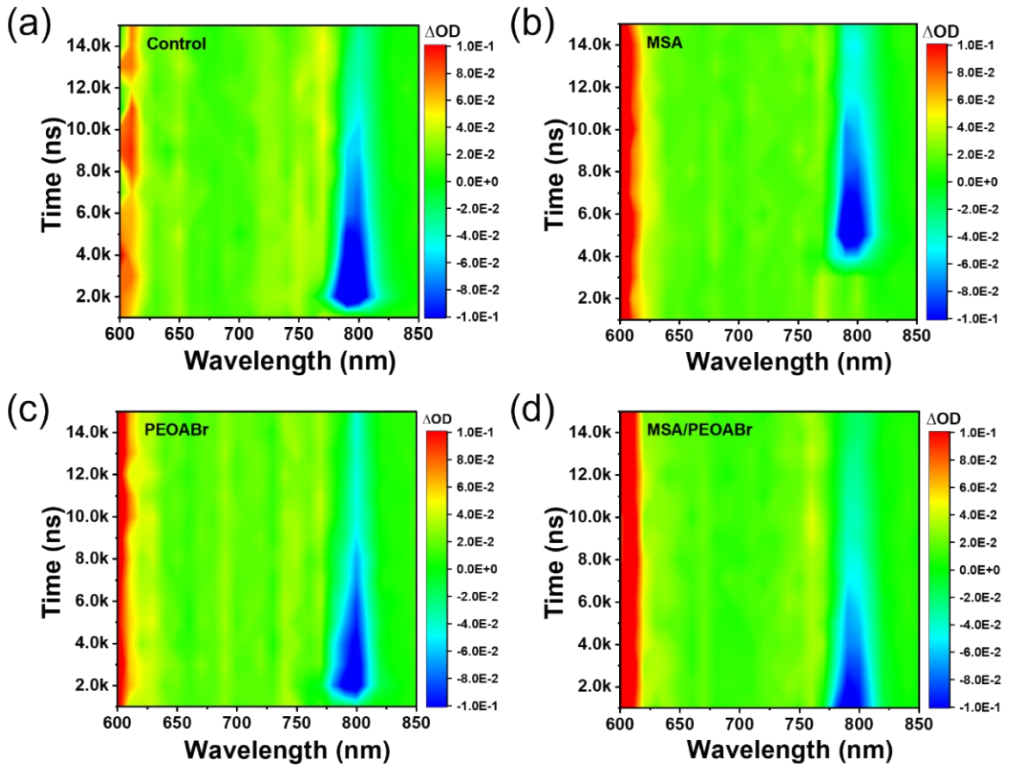


**Figure S7.** Two-dimensional color diagram corresponding to ns-TAS of the perovskite films: a) control; b) MSA; c) PEOABr; d) MSA/PEOABr.

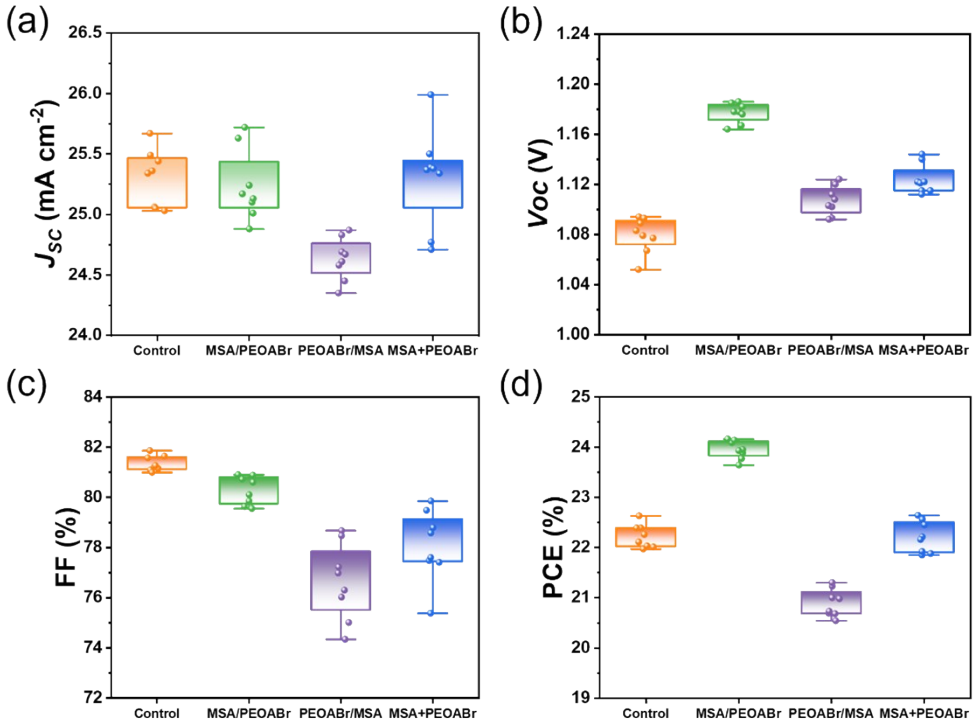


**Figure S8.** Statistical distributions of photovoltaic parameters, including (a) $J_{SC}$, (b)$V_{OC}$, (c) FF and (d) PCE, for devices fabricated by sequential coating (MSA/PEOABr and PEOABr/MSA) and one-step mixed-solution coating (MSA + PEOABr) at different concentrations.

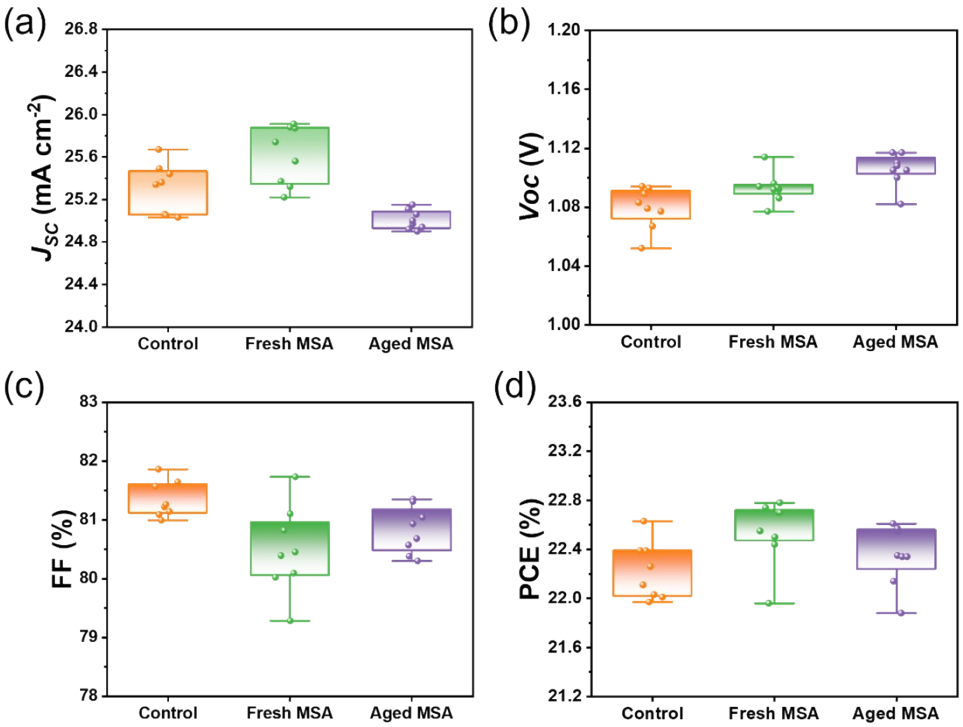


**Figure S9.** Statistical distributions of the photovoltaic parameters for the Control, Fresh MSA, and Aged MSA devices, including (a) $J_{SC}$, (b)$V_{OC}$, (c) FF and (d) PCE.

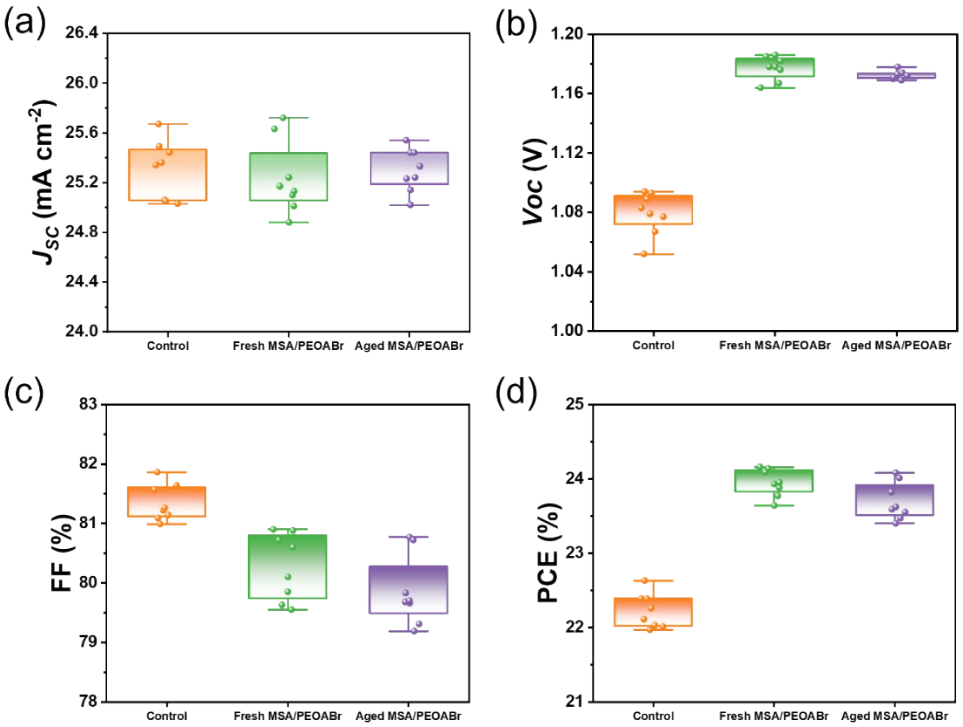


**Figure S10.** Statistical distributions of the photovoltaic parameters for the Control, Fresh MSA/PEOABr, and Aged MSA/PEOABr devices, including (a) $J_{SC}$, (b)$V_{OC}$, (c) FF and (d) PCE.

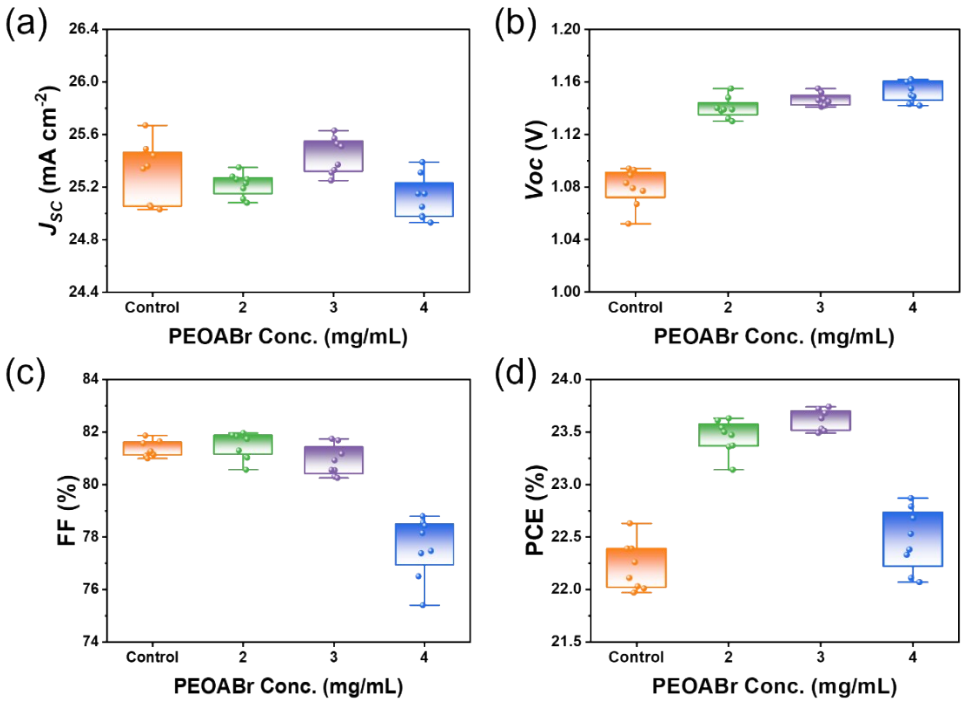


**Figure S11.** Statistical distributions of the photovoltaic parameters (a) $J_{SC}$, (b) $V_{OC}$, (c) FF and (d) PCE, which were quantified at an MSA concentration of 0.5 mg/mL, and the changes in the concentration of PEOABr scaffold device.

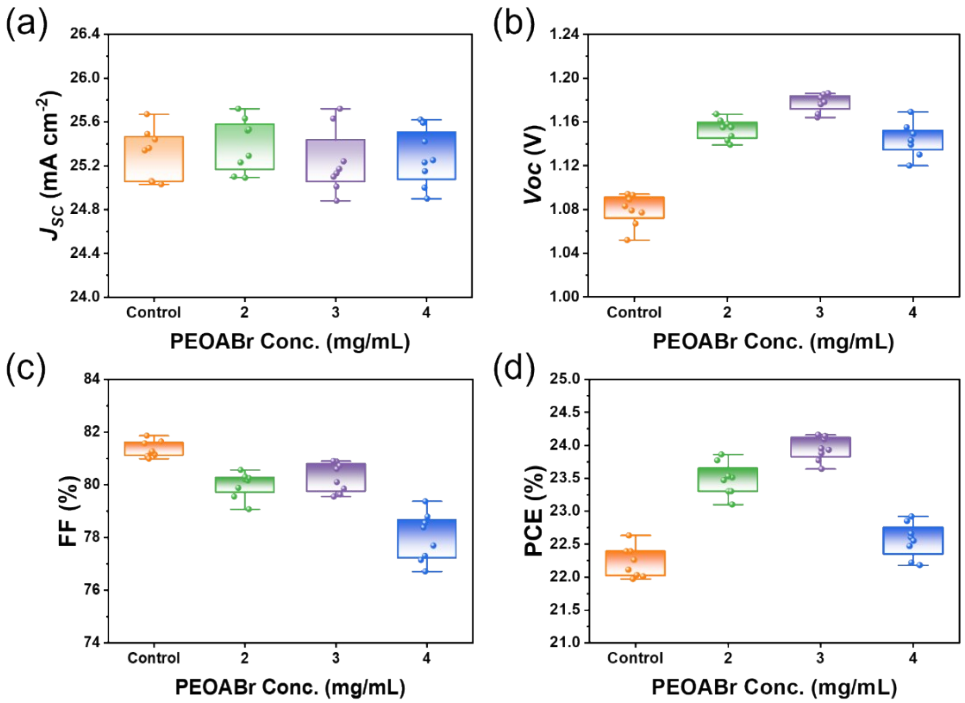


**Figure S12.** Statistical distributions of the photovoltaic parameters (a) $J_{SC}$, (b) $V_{OC}$, (c) FF and (d) PCE, which were quantified at an MSA concentration of 1.0 mg/mL, and the changes in the concentration of PEOABr scaffold device.

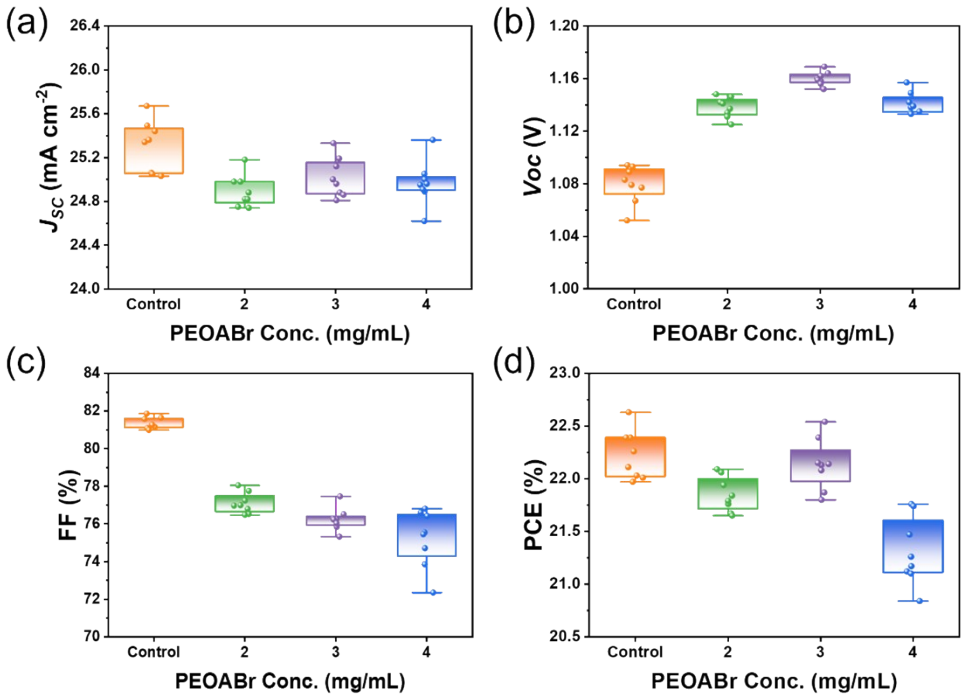


**Figure S13.** Statistical distributions of the photovoltaic parameters (a) $J_{SC}$, (b) $V_{OC}$, (c) FF and (d) PCE, which were quantified at an MSA concentration of 1.5 mg/mL, and the changes in the concentration of PEOABr scaffold device.

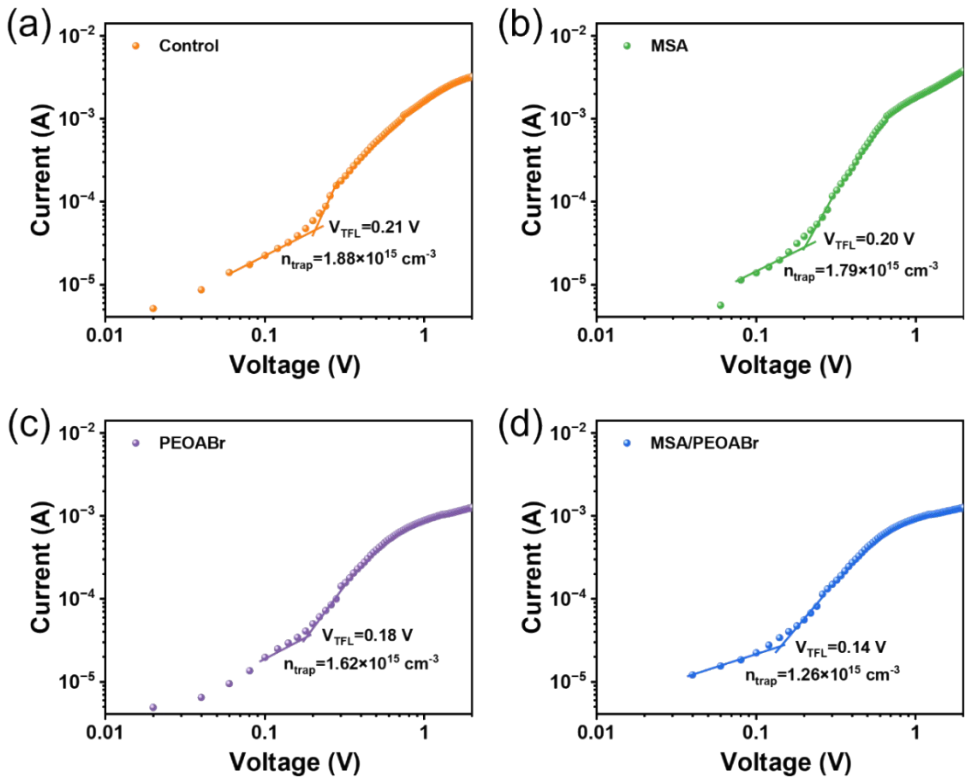


**Figure S14.** a-d) Dark *J–V* characteristics of hole-only devices with the structure ITO/PEDOT:PSS/perovskite (with and without interface treatment using MSA, PEOABr, and MSA/PEOABr/Spiro /Ag**.**

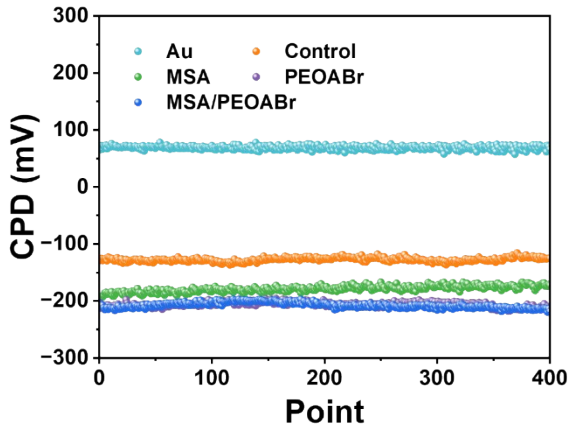


**Figure S15.** Contact potential difference (CPD) measurements of perovskite films with and without interface treatment using MSA, PEOABr, and MSA/PEOABr.

**Table S1.** Fitted results of TRPL decay curves.

| Sample | $A_1$ (%) | $A_2$ (%) | $\tau_1$ (ns) | $\tau_2$ (ns) | $\tau_{ave}$ (ns) |
|---|---|---|---|---|---|
| Control | 43.0 | 57.0 | 111.01 | 514.77 | 459 |
| MSA | 43.0 | 57.0 | 341.95 | 819.16 | 705.71 |
| PEOABr | 3.0 | 97.0 | 178.92 | 721.36 | 716.79 |
| MSA/PEOABr | 41.0 | 59.0 | 557.87 | 1350.25 | 1171.26 |

**Table S2.** Fitted results of TRPL decay curves with Spiro-OMeTAD.

| Sample/Spiro | $A_1$ (%) | $A_2$ (%) | $\tau_1$ (ns) | $\tau_2$ (ns) | $\tau_{ave}$ (ns) |
|---|---|---|---|---|---|
| Control | 43.0 | 57.0 | 1.67 | 229.41 | 228.14 |
| MSA | 44.0 | 56.0 | 8.79 | 161.09 | 154.64 |
| PEOABr | 52.0 | 48.0 | 7.23 | 72.97 | 66.47 |
| MSA/PEOABr | 35.0 | 65.0 | 6.08 | 57.66 | 49.17 |

**Table S3.** Photogenerated resistance parameters extracted from impedance spectra fitting.

| Sample | $R_{ct}$ (KΩ) | $R_{rec}$ (KΩ) |
|---|---|---|
| Control | 12.5 | 110 |
| MSA | 10.5 | 110 |
| PEOABr | 9.56 | 166 |
| MSA/PEOABr | 8.81 | 201 |

**Table S4.** Fitted results of ns-TAS decay curves.

| Sample | $A_1$ (%) | $\tau_1$ (ns) | $A_2$ (%) | $\tau_2$ (ns) | $\tau_{rec}$ (ns) |
|---|---|---|---|---|---|
| Control | 51.43 | 1176.98 | 48.57 | 3085.73 | 2536.59 |
| MSA | 51.19 | 1068.82 | 48.81 | 3648.71 | 3042.33 |
| PEOABr | 57.85 | 1164.85 | 42.15 | 4371.39 | 3512.68 |
| MSA/PEOABr | 65.92 | 1300.49 | 34.08 | 7197.59 | 5670.11 |

**Table S5.** Presents the work function (WF) values calculated from the measured CPD data.

| | Au | Control | MSA | PEOABr | MSA/PEOABr |
|---|---|---|---|---|---|
| $\Phi_{ave}$ (mV) | 70 | -130 | -180 | -200 | -210 |
| WF (eV) | 5.1 | 4.9 | 4.85 | 4.83 | 4.82 |